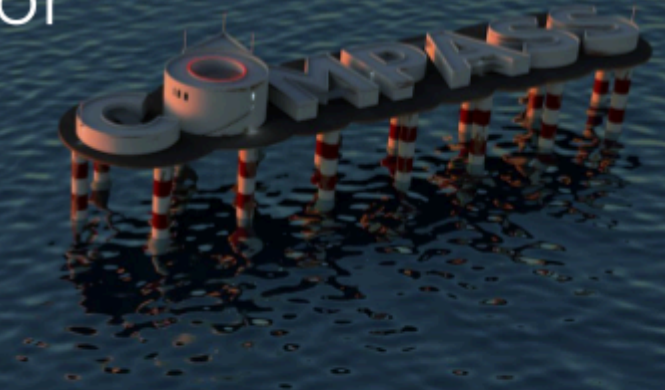


# Tutorial 16 – FDA for Composites

**COMPASSIS**



## Content

---

Content	2
Glossary	4
1. Model description	6
Constraints	7
Materials	7
Local axes	9
Loads	10
Meshing	11
Dynamic data	13
Damping	13
Simulation parameters	14
2. Results	14
Stress results	14
Damage state	18
3. References	19
4. Validation summary	20

(Page left blank intentionally)

## Glossary

---

- FEM: Finite Element Method.
- CAD: Computer Aided Design.
- CAE: Computer Aided Engineering.
- CFD: Computer Fluid Dynamics.
- FRP: Fibre Reinforced Plastic.
- GUI: Graphic User Interface.
- SL-PFEM: Semi Lagrangian Particle Finite Element Method.

(Page left blank intentionally)

## 1. Model description

The present validation case deals with the Fatigue Damage Assessment of composite materials, based on the work of (Joel Jurado-Granados, 2021). The results are compared with the experimental results from (Sandia National Laboratories, n.d.). This methodology implemented in [Tdyn RamSeries](#) is the result of the research conducted on the framework of R+D H2020 [FibreGy project](#) (FibreGy, n.d.).

The benchmark compares the number of cycles at which the specimen fails with the number of cycles at which the failure in the testing campaign appeared.

According to (Joel Jurado-Granados, 2021), the failure in the simulation occurs once the constitutive damage appears in the entire cross section of the specimen, for the load-bearing constituent material. In the current methodology, the criteria are analogous. According to the Palmgren-Miner rule, the nucleation of failure will appear once the fatigue damage (Palmgren damage) reaches value of one,  $d = 1.0$ .

The dimensions of the specimen are in agreement with the experimental results, as well as the numerical results presented in (Joel Jurado-Granados, 2021). In the next picture, the dimensions are shown:

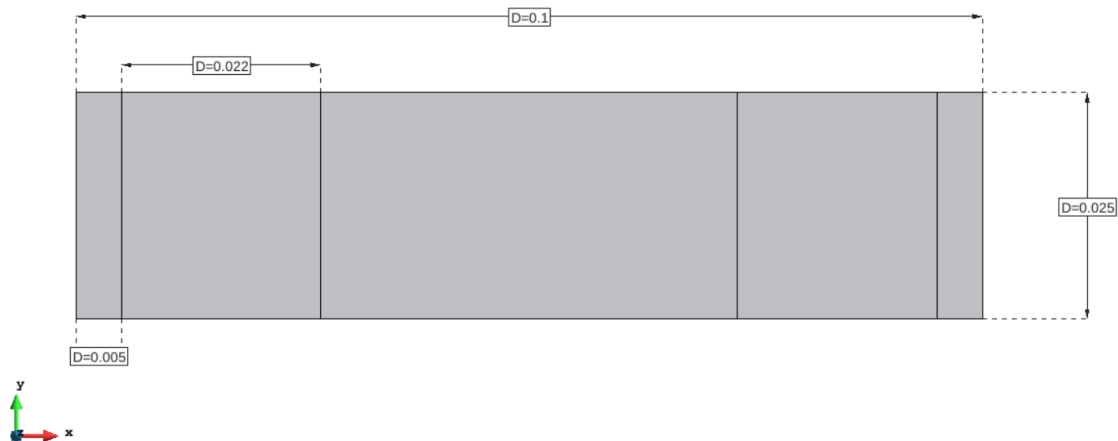


Figure 1: Specimen/model dimensions.

The specimen thickness is  $t = 2.7mm$ .

As in the case of (Joel Jurado-Granados, 2021), two zones of length  $l = 0.005m$  have been defined. These zones belong to the near end of the specimen, where the specimen is fixed. The reason to define such zones is to avoid numerical stress concentrations. Besides, two zones of length  $l = 0.022m$  were defined, in which mesh will be refined in order to obtain a better definition of the stress gradients.

The test specimen is subjected to a sinusoidal load cycle of stress ratio  $R = 0.10$ , as in the experimental testing. Four stress levels are evaluated:  $27MPa$ ,  $24MPa$ ,  $21MPa$ ,  $19MPa$ , in the central cross section. The number of cycles at which the failure is produced for each stress level is compared with the experimental SN curve. In the next figure is shown the edge where the load is applied:

## Constraints

The specimen is clamped on one end, and on the opposite only displacement in  $X$  direction is allowed. The boundary conditions are shown in the next figure:

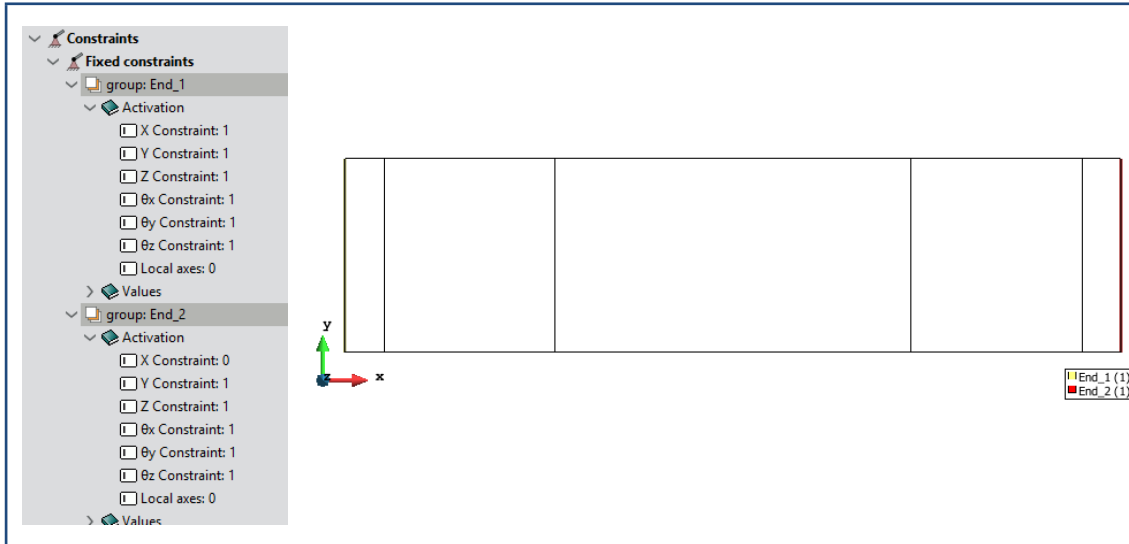


Table 1: Boundary conditions

## Materials

The laminate is compound of six orthotropic layers. Each layer is oriented according to the  $[\pm 60]_3$  stacking sequence and made of the same material. The definition of the laminate is shown in the figure below:

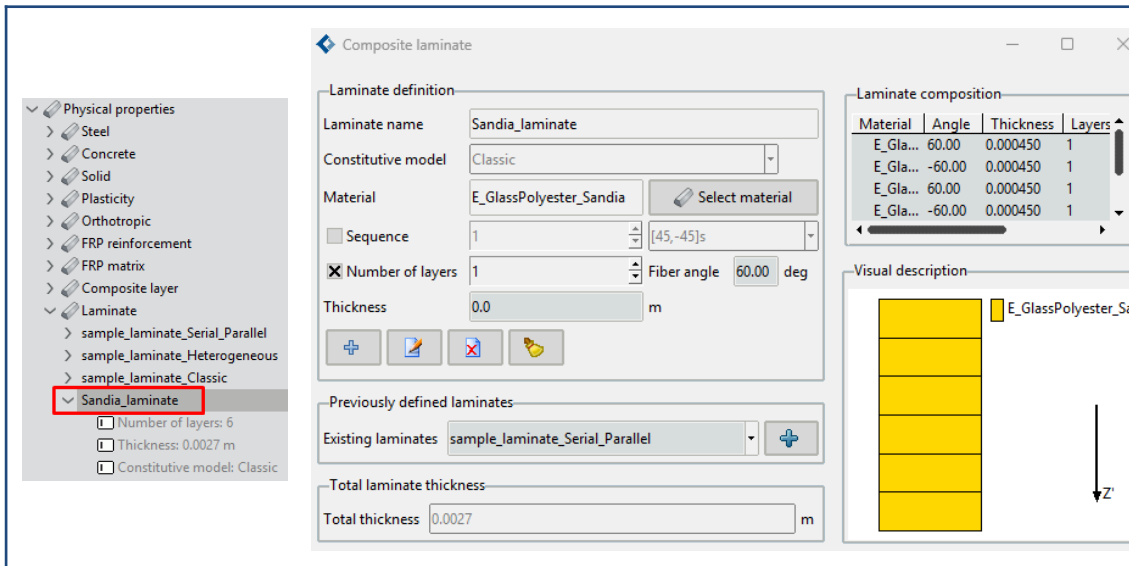


Table 2: Laminate's definition window. In this case, the laminate consists on a balanced angle ply laminate

The laminate is created from plies of a material assumed linear elastic, with the following properties:

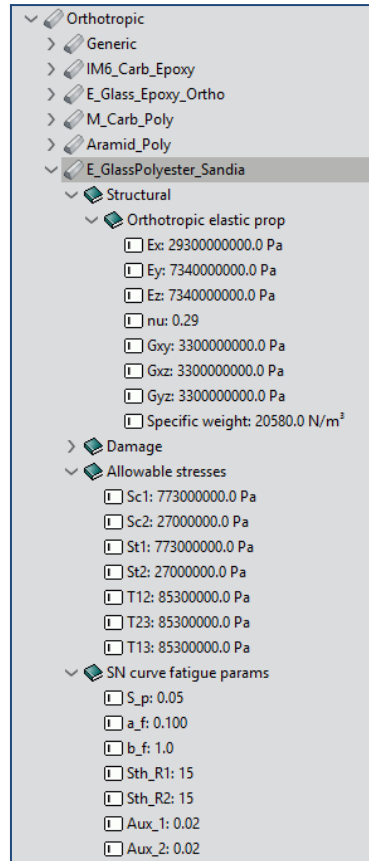


Figure 2: Ply material introduced as orthotropic

$E_x$ [Pa]	$E_y$ [Pa]	$E_z$ [Pa]	$G_{xy}$ [Pa]	$G_{xz}$ [Pa]	$G_{yz}$ [Pa]	$\nu$
2.93e10	0.734e10	0.734e10	0.33e10	0.33e10	0.33e10	0.29

Table 3: Mechanical properties of the ply material (Uni-Directional).

Strength properties:

$\sigma_x^c$ [Pa]	$\sigma_x^t$ [Pa]	$\sigma_y^c$ [Pa]	$\sigma_y^t$ [Pa]	$\tau_{xy}$ [Pa]	$\tau_{xz}$ [Pa]	$\tau_{yz}$ [Pa]
7.73e8	7.73e8	0.27e8	0.27e8	0.853e8	0.853e8	0.853e8

Table 4: Strength properties of the ply material (UD) (allowable stresses).

And the fatigue parameters, according to matrix failure (Joel Jurado-Granados, 2021):

$\alpha_f$	$\beta_f$	STHR	Aux	$S_e/S_u$
0.100	1.0	15	0.02	0.05

Table 5: Fatigue parameters





## Tutorial 16 - FDA for Composites.

The same laminate material has been assigned to different zones of the specimen, in order to set the zones where fatigue damage is to be assessed.

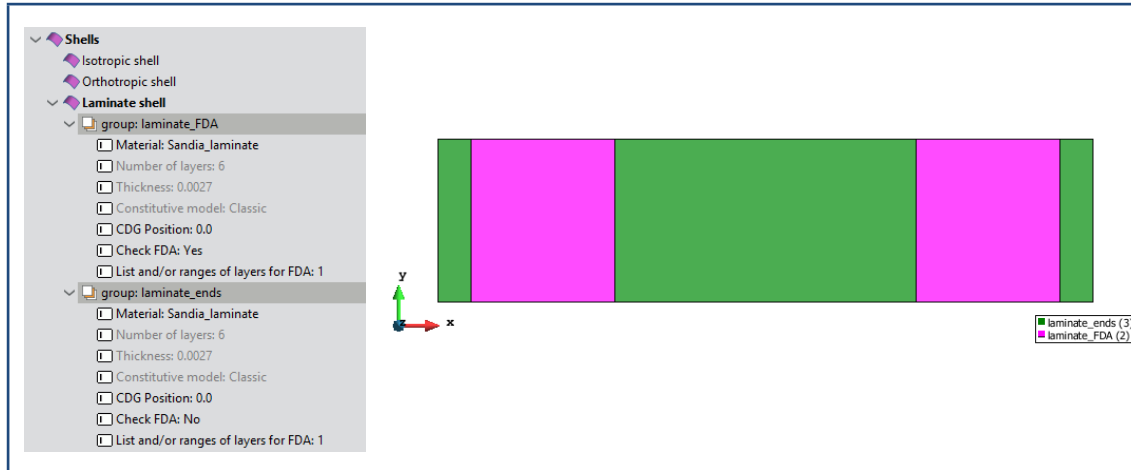


Table 6: Different assigned zones of the model (same laminate), for damage assessment

## Local axes

Local axes have been defined to properly characterise the anisotropic properties of the laminate. In particular, the local axes of the shell coincide with the global axes of the model. By this means, the X local axe coincides with the longitudinal direction of the specimen, as well that represents the reference for the laminate angles ( $0^\circ$  direction).

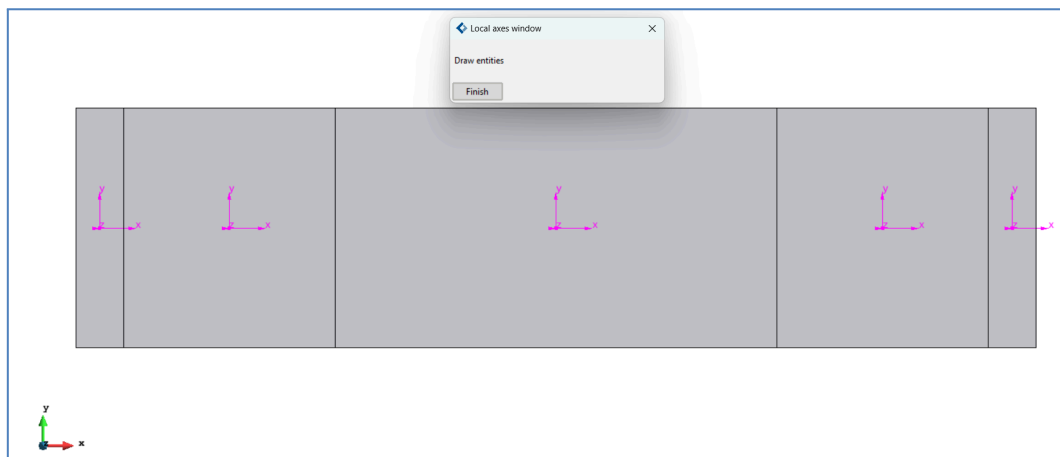


Figure 3: Local axes definition.

## Loads

As mentioned, a sinusoidal load is applied. This load is defined as a factor of  $A = 0.55 + 0.45 \cdot \sin(\omega t)$ . By this means, the factor for minimum stress is 0.10, and the maximum is 1.0, maintaining the stress ratio  $R = \frac{\sigma_{min}}{\sigma_{max}} = 0.10$ .

The load applied is to obtain the targeted stress levels, which belongs to the maximum stress applied in each cycle.

The load level is applied by defining a boundary pressure load in the shell. The corresponding values for each stress level are shown next:

Stress level [MPa]	19	21	24	28
Load level [N/m]	51300	56700	64800	75600

Table 7: Load levels applied according to stress level desired.

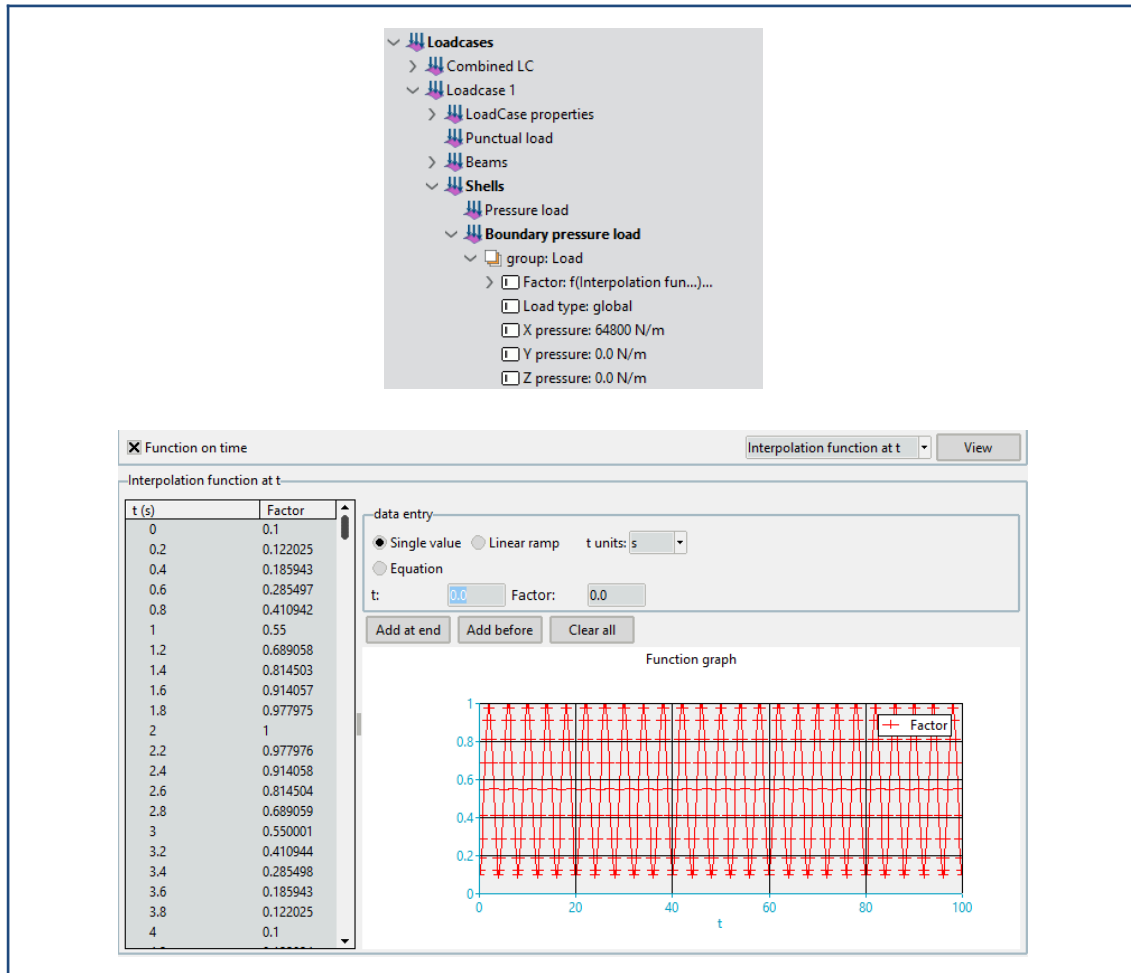


Table 8: Cyclic loading definition

## Meshing

Symmetrical structural mesh of triangle elements has been used. The size of the elements has been chosen after conducting a mesh convergence analysis.

Consequently, three different mesh sizes were compared. The mesh size was in function of defining the number of divisions in each surface, as it is depicted in Table 9

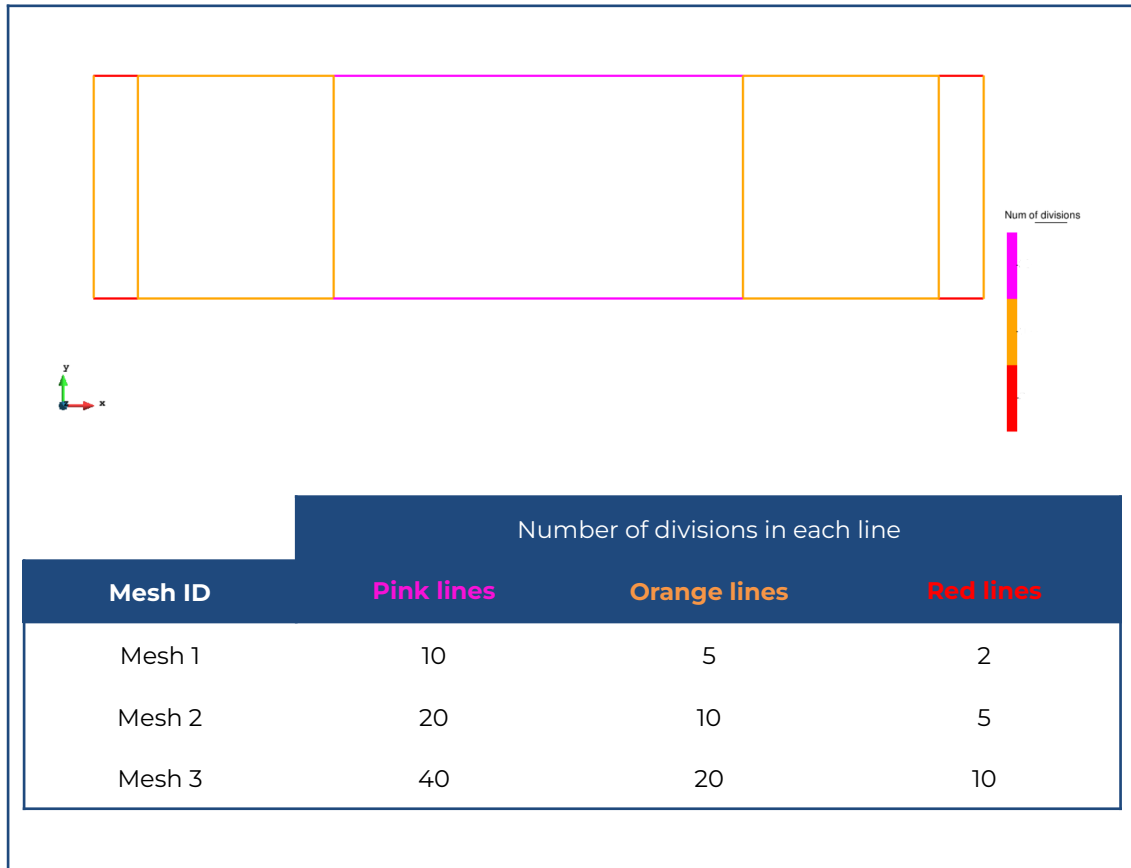


Table 9: Size definition for mesh convergence study

The parameters for each mesh are shown next.

Mesh name	Nº elements	Nº of nodes
Mesh 1	480	270
Mesh 2	2000	1061
Mesh 3	8000	4121

Table 10: Mesh parameters of the mesh convergence study.

The chosen result for checking the mesh convergence is the displacement in X direction of the specimen. The selected point is located in the middle of the width of the specimen (as it is shown in Figure 4).

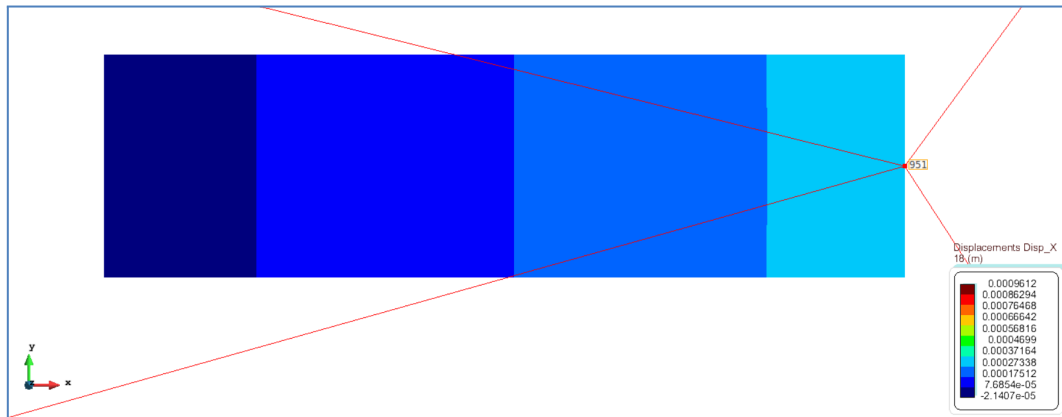


Figure 4: Reference point for studying mesh convergence.

The results of the mesh convergence study are shown on Table 11. From these results, it is appreciated that mesh definition does not interfere on the results obtained. Finally, the mesh chosen for this simulation is Mesh 3, to better obtain the stress distribution across the specimen, while keeping the number of elements reasonable. The final mesh is shown on Figure 5.

Mesh ID	Result (displacement X) [mm]	Difference [%]
Mesh 1	0.2966	-
Mesh 2	0.297	0.135%
Mesh 3	0.2971	0.034%

Table 11: Results of the mesh convergence study.

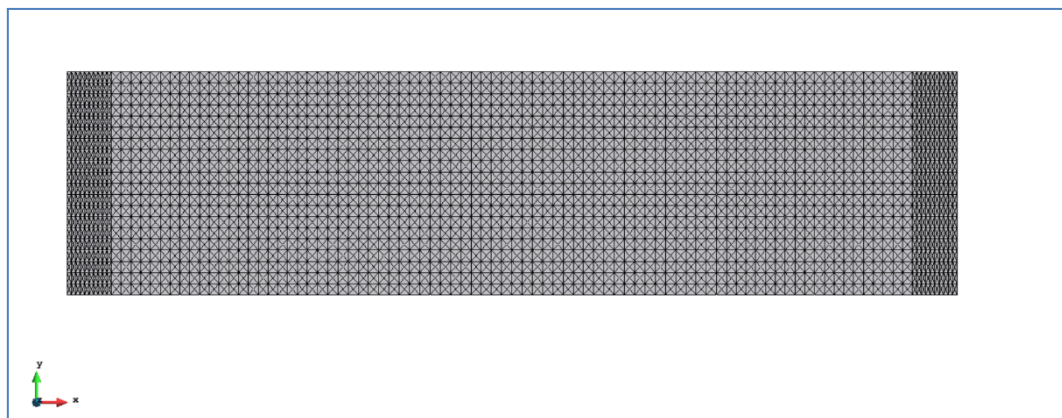


Figure 5: Final mesh used.

## Dynamic data

### Damping

The damping data used is the following:

<b>Damping type</b>	Rayleigh damping
<b>Damping ratio</b>	0.032
$\alpha_M$ (mass damping)	0.1005
$\alpha_K$ (stiffness damping)	1.831E-05

Table 12: Damping data.

The damping coefficients have been calculated to obtain a damping ratio of 3.2%, being the first natural frequency  $f_1 = 556\text{Hz}$  and external load frequency  $f_{ext} = 0.25\text{Hz}$ .

The value of the damping ratio has been obtained by extrapolating data from literature. According to (V. P. Eremin, May 2023) and (K. Diharjo, 2018), the damping ratio depends on the type of matrix, fibre and volumetric participation of fibre. For a laminate based on fibre glass epoxy system, the following results were displayed:

<b>Fibre participation, <math>V_f</math> [%]</b>	15	20	25	30	35
<b>Damping ratio [%]</b>	3.90	3.80	3.70	3.50	3.40

Table 13: Damping ratio in function of fibre participation (K. Diharjo, 2018).

A lineal performance of such data can be supposed, as it is shown in the next figure. By this means, the damping ratio can be obtained for 37% of volumetric fibre participation, which corresponds to testing data.

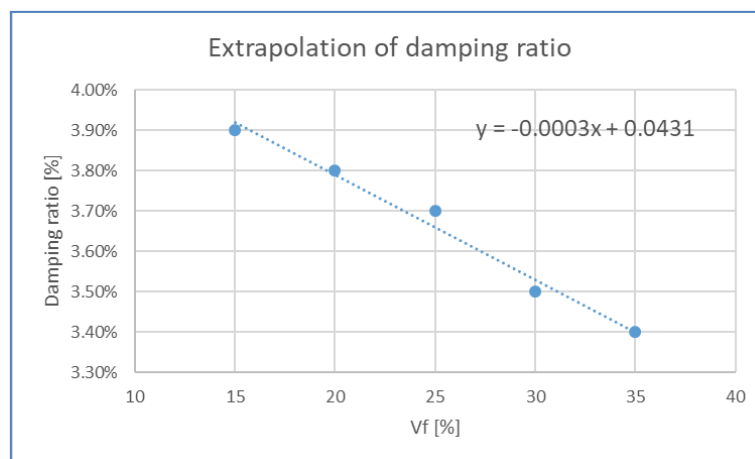


Figure 6: Linearization of damping ratio in function of fibre participation (K. Diharjo, 2018).

According to the figure above, the damping ratio is 3.2% for a fibre participation of  $V_f = 37\%$ .

Therefore, the damping coefficients are defined following:

$$\alpha_K = \frac{2\xi}{(\omega_1 + \omega_{ext})} = 1.831 \cdot 10^{-5}$$

$$\alpha_M = \alpha_K \cdot \omega_1 \cdot \omega_{ext} = 0.1005$$

Being  $\omega_1$  the first natural frequency in  $rad/s$  and  $\omega_{ext}$  the external load frequency in  $rad/s$ .

### Simulation parameters

In the next table, the simulation parameters used are shown:

$\Delta t$ [s]	$N_{steps}$	$T_{total}$	$T_{out}$
0.2	500	100	20

Table 14: Simulation parameters.

The time increment was selected to accurately resolve the applied sinusoidal load. As a rule of thumb, at least 10–20 integration points per period are required to capture a sinusoid without phase distortion or amplitude aliasing.

The total duration was chosen to observe the decay of initial transients and the establishment of steady-state response under harmonic excitation.

## 2. Results

### Stress results

The stress field ( $\sigma_x$ ,  $\sigma_y$ ,  $\sigma_{xy}$ ) of the laminate for the first ply is shown in the next image. The stress field verification for composite laminates in Tdyn RamSeries is demonstrated in a previous validation case. For more information, visit [COMPASSIS webpage](http://www.compassis.com).

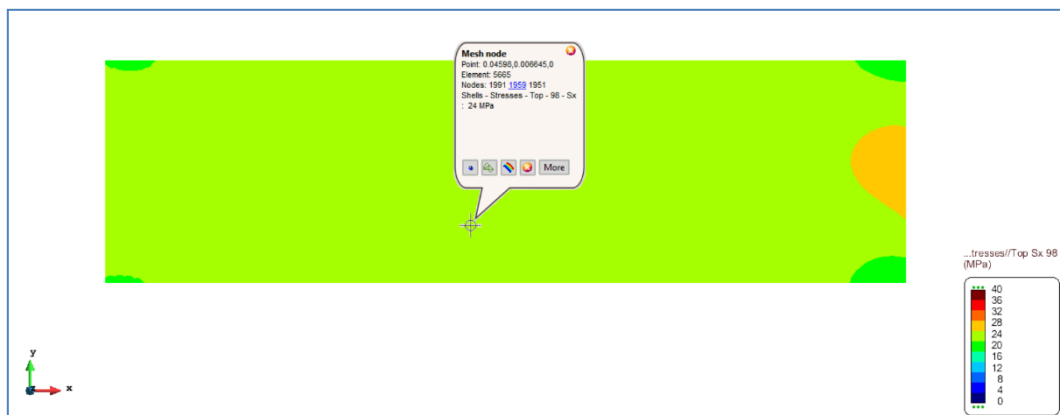


Figure 7:  $S_x$  of the laminate. According to 24 MPa.

In Table 15, the stress components respect to ply axes (fibre direction,  $\sigma_1$ , perpendicular to fibre,  $\sigma_2$ , shear component,  $\sigma_{12}$ ) are shown. These components are used to calculate the equivalent UD90 stress (defined in Equation 1).



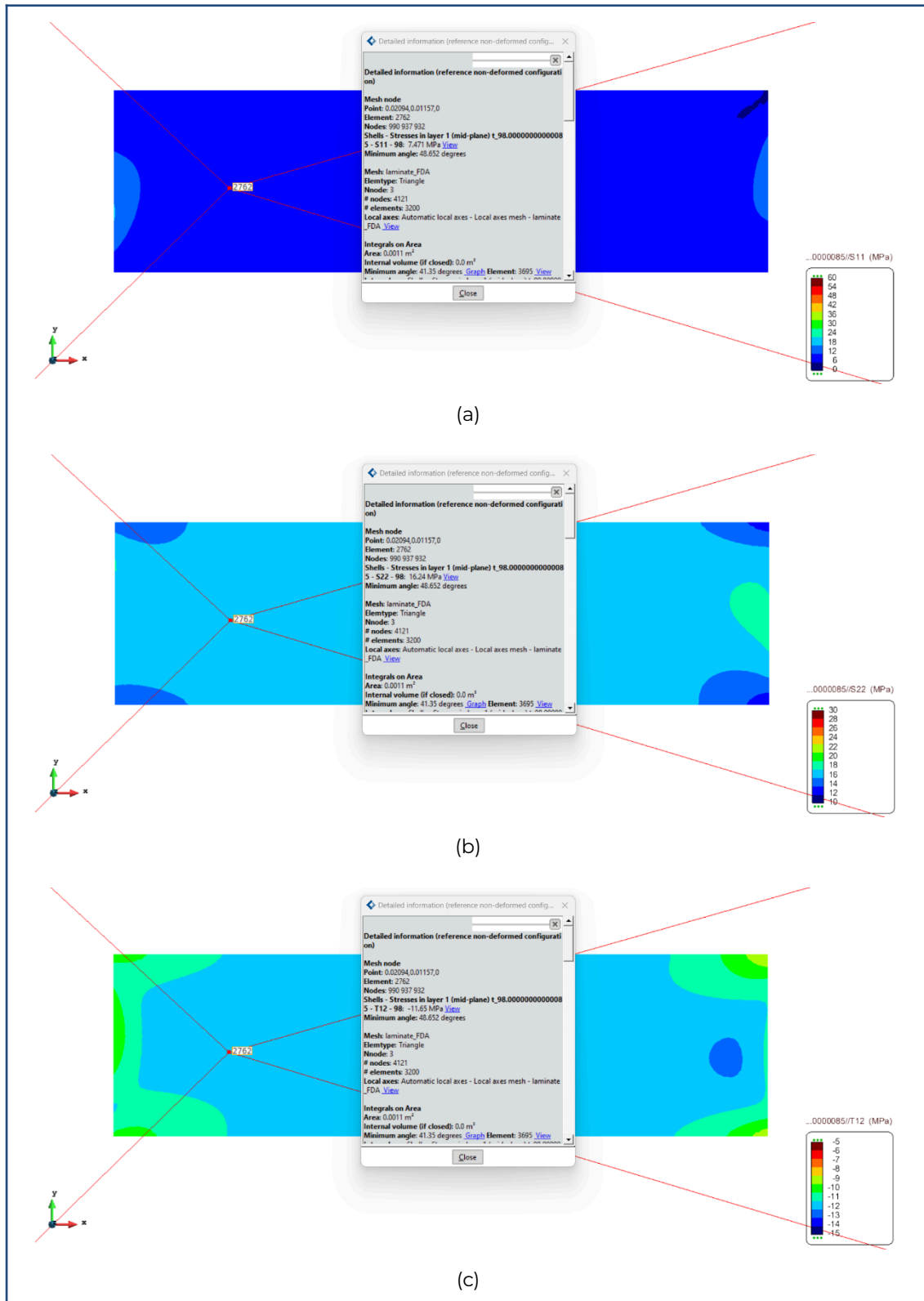


Table 15: Stress field results for ply 1. (a)  $S_{11}$ . (b)  $S_{22}$ . (c)  $S_{12}$ .



According to this stress state, the equivalent matrix stress is:

Equation 1

$$\sigma_{eq,UD0} = \sqrt{\sigma_2^2 + f_{12}^2 \cdot \sigma_{12}^2} = \sqrt{16.24^2 + (-11.65 \cdot f_{12})^2}$$

Which fulfils the computed equivalent stress:

$$\sigma_{eq,UD90} = 16.65 \text{ MPa}$$

Where  $f_{12} = \sigma_2^t / \tau$ , being  $\sigma_2^t$  the transverse tensile strength of the ply, and  $\tau$  the shear strength of the ply.

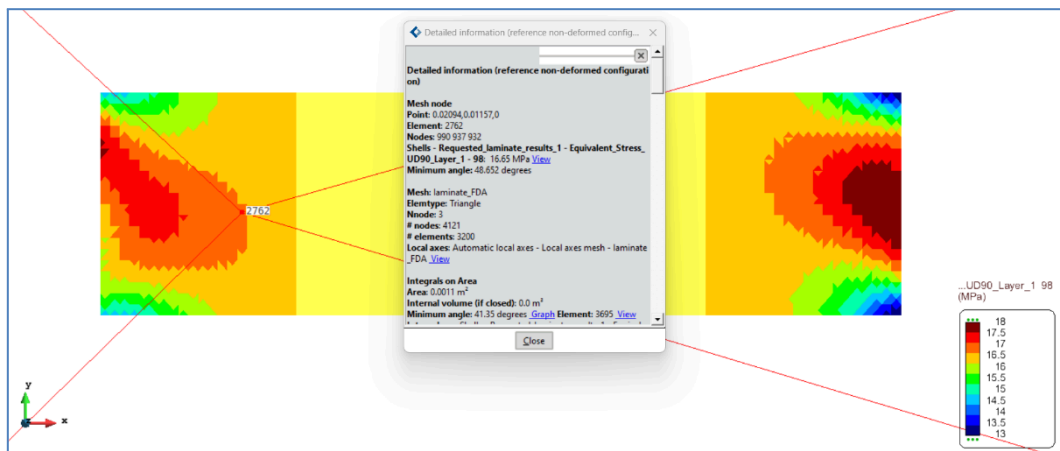


Figure 8: Equivalent UD90 stress on the specimen.

In the next figure, the evolution in time of the equivalent UD90 stress is shown. As it is seen, the maximum stress in each cycle is 16 MPa.

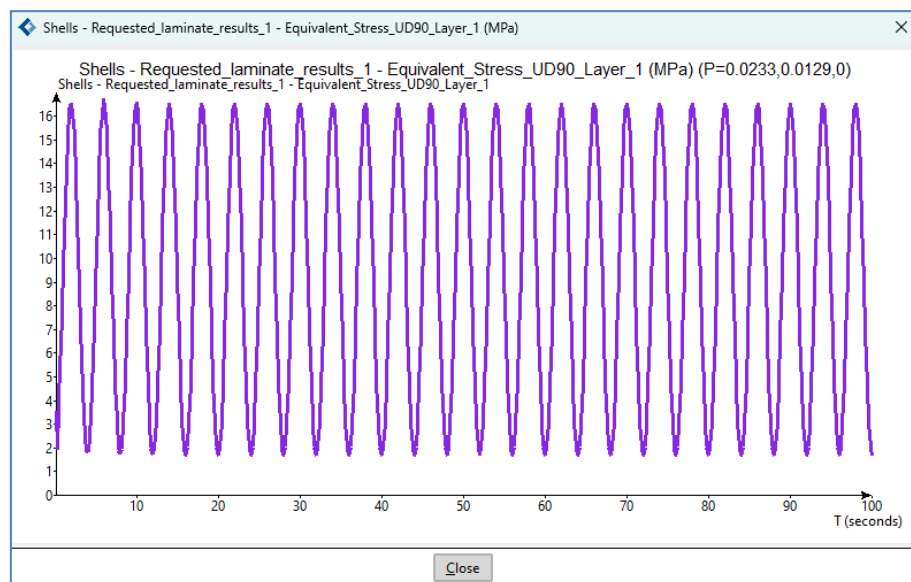


Figure 9: Equivalent UD90 stress evolution over time.

From the picture above, the expected result of number of cycles after applying Pagoda Rainflow Counting method is 25 cycles. Therefore, to extend the number of cycles applied, higher time simulation should be conducted. However, it can be achieved by defining a value for *Total Time* in the loading case parameter, according to the desired number of cycles to achieve. However, the first seconds of the simulation are discarded by initializing the cyclic counting since step time 20s (*Initialization time* in Figure 10), in order to avoid transient effects at the beginning of the simulation. Hence, the total number of cycles computed by the Rainflow Counting Method is  $n_{sim} = 20$  cycles.

In the case of stress level of 24MPa, the Total Time is defined as  $t_{tot} = 131555s$ , corresponding to 26311 cycles. The number of cycles is computed following the expression:

$$N = \frac{Tot_{time}}{Sim_{time}} \cdot n_{sim}$$

Being  $Sim_{time} = 100s$ , as the simulation time.

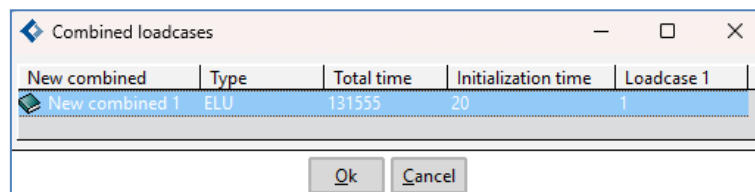


Figure 10: Total time simulation (case of 24MPa).

## Damage state

The damage state (Palmgren-Miner) is the following:



Figure 11: Damage state after 26311 cycles (24MPa).

In accordance to reference (Joel Jurado-Granados, 2021), the failure of the specimen is obtained once constitutive damage (V. P. Eremin, May 2023) appears in the whole cross-section of the specimen. This is equivalent to obtain Palmgren-Miner damage equal to 1.0 across the whole cross-section of the specimen, as it is depicted in Figure 11.

According to the results, the SN curve of the laminate is shown in the next figure, comparing the experimental results from literature (Sandia National Laboratories, n.d.), the numerical results from (Joel Jurado-Granados, 2021), and the results obtained by Tdyn RamSeries.

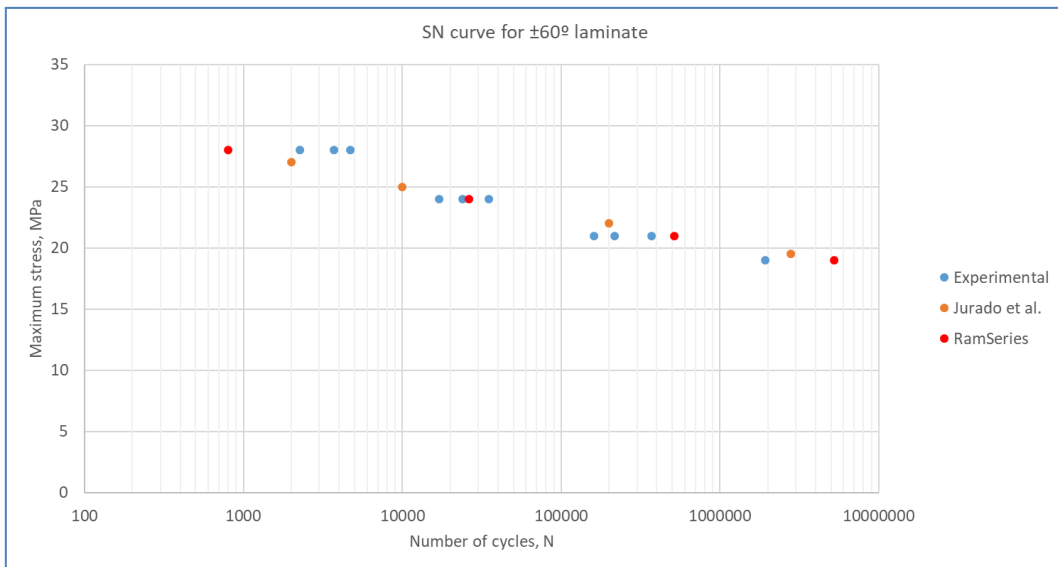


Figure 12: SN curve, comparing the experimental results, Tdyn RamSeries results, and literature results.

### 3. References

- CEN. (2003). Eurocode 1: Actions on structures - Part 1-3: General actions - Snow loads.
- CEN. (2005). Eurocode 3: Design of steel structures - Part 1-1: General rules and rules for buildings.
- CEN. (2005). Eurocode 3: Design of steel structures - Part 1-4: General rules - Supplementary rules for stainless steels.
- CEN. (2005). Eurocode: Basis of structural design.
- CEN. (2010). Eurocode 1: Actions on structures - Part 1-4: General actions - Wind Actions.
- Compass. (s.f.). *Tdyn CFD + HT Reference*. Obtenido de Compass IS: <http://www.compassis.com/downloads/Manuals/TdynReference.pdf>
- Compass. (s.f.). *Turbulence Handbook*. Obtenido de Compass IS: <http://www.compassis.com/downloads/Manuals/TdynTurbulenceHB.pdf>
- CompassIS. (s.f.). *CompassIS products Tdyn CFD+HT*. Obtenido de Compass IS: <http://www.compassis.com/compass/en/Productos/Tdyn+CFD%2BHT>
- CompassIS. (s.f.). *CompassIS products Tdyn RamSeries*. Obtenido de Compass IS: <http://www.compassis.com/compass/en/Productos/RamSeries>
- CompassIS. (s.f.). *RamSeries reference manual*. Obtenido de CompassIS: [http://www.compassis.com/downloads/Manuals/Ramseries\\_Reference\\_Manual.pdf](http://www.compassis.com/downloads/Manuals/Ramseries_Reference_Manual.pdf)
- FibreGy. (s.f.). Recuperado el 10 de June de 2025, de <https://fibregy.eu/>.
- Joel Jurado-Granados, X. M. (2021, July 1). Fatigue prediction of composite materials, based on serial/parallel mixing theory. *Composite Structures*, 291, 115516. doi:10.1016/j.compstruct.2022.115516
- K. Diharjo, D. D. (2018). Vibration-Damping Factor of Glass/Kenaf/Polyester Hybrid Composite. *Vol. 772*(pp 38-42).
- Ltd, A. (s.f.). Green House Analysis Rev. A.
- Sandia National Laboratories. (s.f.). Recuperado el 10 de June de 2025, de <https://energy.sandia.gov/programs/renewable-energy/wind-power/rotor-innovation/rotor-reliability/mhk-materials-database/>
- V. P. Eremin, E. G. (May 2023). Identification of the parameters of a composite material. 25(3). Retrieved from <https://www.extrica.com/article/22670/pdf>

#### 4. Validation summary

---

CompassFEM versión	16.6.2
Tdyn solver versión	16.6.2
Ramseries solver versión	16.6.2
Benchmark status	Successful
Last validation date	22/08/2025